J1.3   STUDY ON OUTDOOR THERMAL ENVIRONMENT AROUND COOLING TOWERS OF
LARGE DISTRICT HEATING AND COOLING SYSTEM IN SUMMER IN TOKYO
- FIELD MEASUREMENT AND COUPLED SIMULATION OF CONVECTION, RADIATION AND CONDUCTION -

Hong HUANG*, Ryozo OOKA, Shinsuke KATO
Institute of Industrial Science, The University of Tokyo, Japan

1. INTRODUCTION

Outdoor thermal environment represented by the urban heat island phenomenon has become markedly worse in recent years due to the change in land covering and the increase in the artificial heat release that accompanies urbanization. The heat released by air conditioning is thought to be one of the factors in the deterioration of the outdoor thermal environment. A large number of District Heating and Cooling Systems (DHC) have been introduced into large cities, such as Tokyo, in Japan. As the heat loads of the buildings supplied by the system are released together from the DHC system's cooling towers in the summer, it is necessary to ensure that the method used to discharge this heat has a minimum influence on the outdoor thermal environment around these cooling towers. In this study, in order to clarify the influence of the DHC system's cooling towers on the outdoor thermal environment around the DHC system in the summer: 1) the actual situation of the outdoor environment around the Shinjuku DHC center (next to Shinjuku Park Tower, a 52-storey building), which has the largest cooling capacity in the world (cooling capacity: 207,680kw; supplied floor space: 2,200,000 m^2; eight cooling towers) is investigated from field measurement; 2) a simulation program for the thermal environment adapted to an unstructured computational grid and which is suitable for complex urban areas coupled with convection, radiation and conduction is developed based on a thermal environment evaluation method (Harayama, 2002; Yoshida, 2000a; Yoshida, 2000b). The spatial distributions of wind velocity, air temperature, and humidity in the area where the field measurement were made are analyzed by the simulation program. The numerical results are compared to the field measurement in order to confirm the accuracy of the simulation program. The influence

* *Corresponding author address:* Hong Huang,
Institute of Industrial Science, The University of Tokyo,
4-6-1 Komaba, Meguro-ku, Tokyo, 153-8505, Japan
email: hhong@iis.u-tokyo.ac.jp

of the cooling towers on the outdoor environment is analyzed. Furthermore, the spatial distributions of SET* (Standard Effective Temperature) is also calculated using the above results to estimate thermal comfort at pedestrian level.

2. OUTDOOR THERMAL ENVIRONMENT SIMULATION METHOD

A simulation method coupled with three-dimensional Computational Fluid Dynamics (CFD) analysis, three-dimensional radiation analysis, and one-dimensional heat conduction analysis (Harayama, 2002; Yoshida, 2000a; Yoshida, 2000b) is used to assess the outdoor thermal environment. Figure 1 shows the flowchart for this method. First, boundary conditions are set up from various input conditions. Second, a three-dimensional radiation calculation based on the Monte Carlo method is performed. Then, the temperature distribution inside the ground or wall is calculated by solving an unsteady one-dimensional heat conduction equation. Three-dimensional coupled convection and water vapor transportation calculations are performed continuously by adding new boundary conditions for the surface temperature distribution of the ground and wall and air-conditioning heat load obtained from the radiation and conduction calculation. The coupled simulation of convection, radiation and conduction is then completed by repeating these operations in series. The spatial distribution of the wind velocity, air temperature, humidity, and MRT (Mean Radiant Temperature) are calculated using this coupled simulation. Finally, the spatial distribution of SET*, the comprehensive index of human thermal comfort, is calculated by assuming the amount of clothes and metabolism of the human body. SET * is calculated by the program based on the human thermal equilibrium model of Gagge et al. (1986).

However, this tool had been adapted only for a structured computational grid up to now. Because the buildings around the Shinjuku DHC center have various shapes and geographical features are very complex, if a structured grid is used, it is not only a
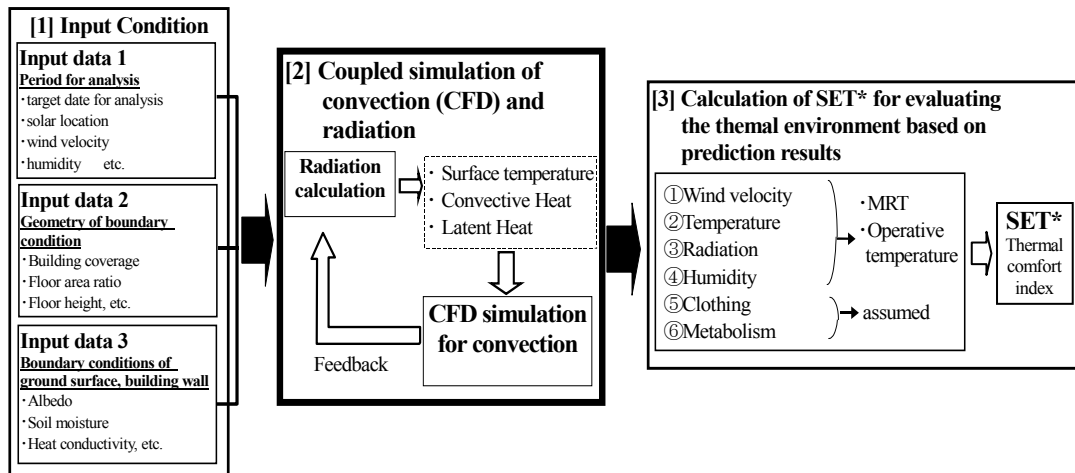
Fig.1 Flowchart for assessing outdoor thermal environment based on coupled simulation of convection, radiation and conduction
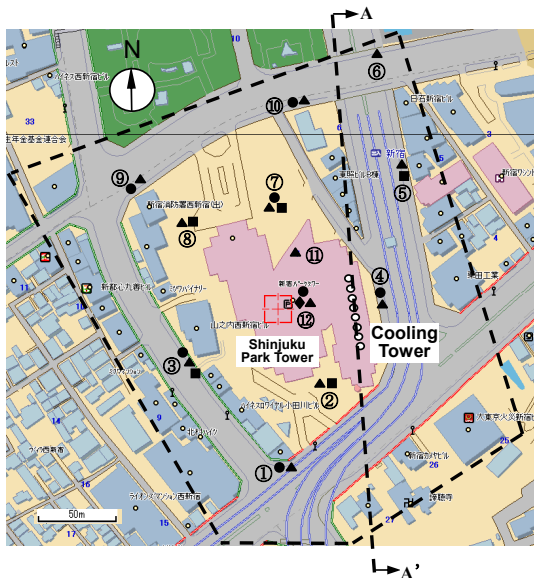
▲Air Temperature, Humidity Measurement Points (12 points)
●Wind Direction, Velocity Measurement Points (7 points)
■Wall, Ground Temperature Measurement Points (5 points)
◆Total Solar Measurement Points (1 points)

Fig.2 Measurement and analysis field
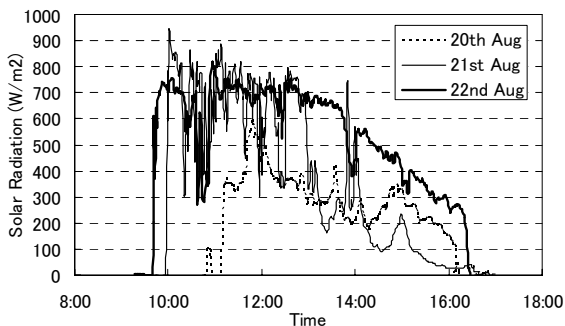
Fig.3 Solar radiation

time-consuming job to construct, but also it is difficult to express the complex urban area accurately with the grid. The use of an unstructured computational grid is effective in carrying out a CFD analysis of such a

Table 1 Field measurement items

No.	Measurement Item	Measuring Equipment
1	Solar radiation	Pyranometer
2	Direction and velocity of wind	Hot wire anemometer+flag
3	Air temperature and humidity	Temperature/Humidity recorder
4	Surface temperature	Thermocouple+Data recorder
		Infrared radiation thermometer

complex urban area. In this study, this tool has been entended to adapt it for an unstructured computational grid suitable for the complex urban area. An approach that Omori (2003) developed was used for the treatment of the unstructured grid. The commercial CFD code Star-CD was used for the CFD calculation.

3. OUTLINE OF FIELD MEASUREMENT AND RESULTS

3.1 Outline of Field Measurement

The object of measurement covers a range of about 200m in radius to the center of the Shinjuku DHC center, and the measurement time is 10:00-16:00 each day on 20th to 22nd August, 2003. The velocity and direction of the wind, the temperature, the humidity, and the temperatures of the ground and the building wall were measured at several points in the area. Figure 2 shows the measurement items and the measurement positions. Table 1 shows the measurement items and the measurement equipment. Meteorological conditions (velocity of the wind, temperature, and humidity) during the measurement period were measured on the rooftop (measurement point 12, 52nd floor above ground, and 220m in height) of the Shinjuku Park Tower. The measurement
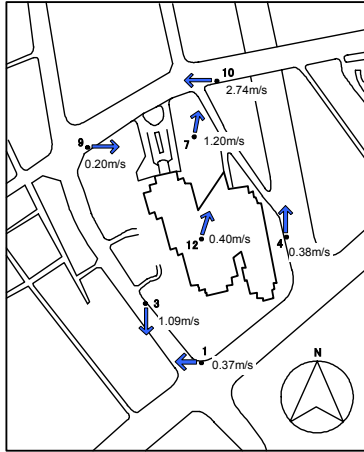
Fig. 4 Wind distribution (10:00, 22nd Aug)
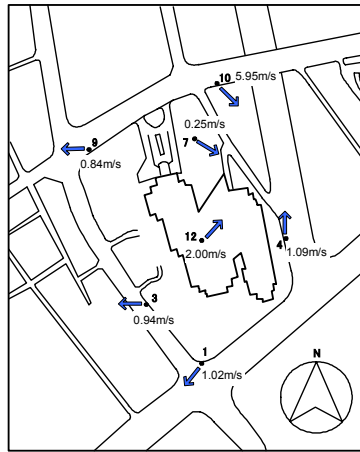
Fig. 5 Wind distribution (13:00, 22nd Aug)
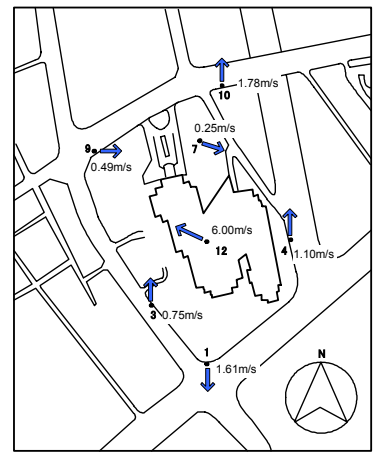
Fig. 6 Wind distribution (15:00, 22nd Aug)
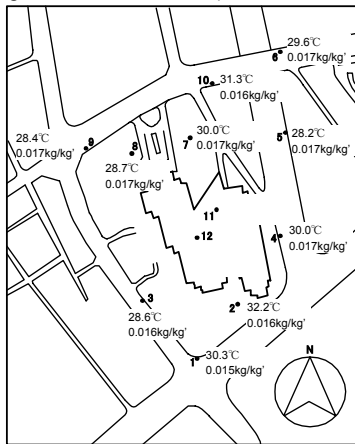
Fig. 7 Temperature and humidity
(10:00, 22nd Aug)
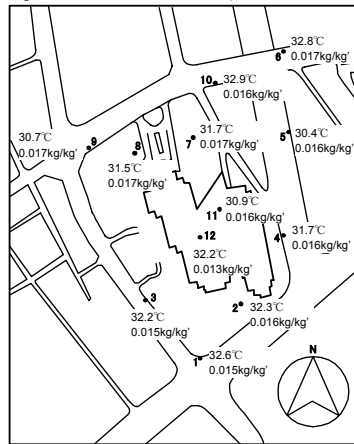
Fig. 8 Temperature and humidity
(13:00, 22nd Aug)
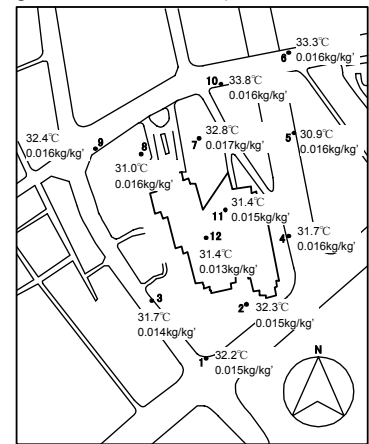
Fig. 9 Temperature and humidity
(15:00, 22nd Aug)
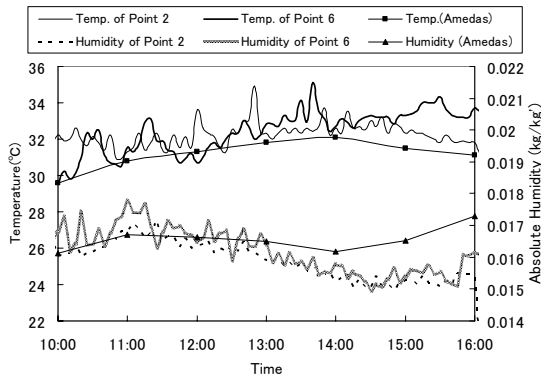
Fig. 10 Time history for temperature and humidity (22nd Aug.)
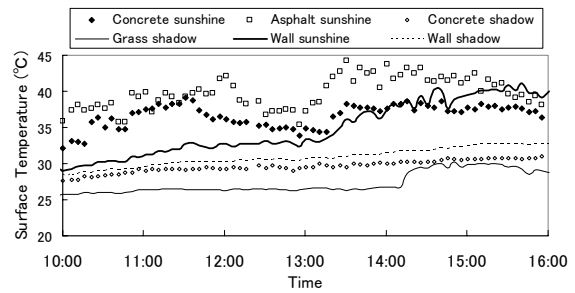
Fig. 11 Wall temperature (22nd Aug.)

heights for the velocity of the wind, temperature, and humidity are all 1.5m above the ground excluding the Shinjuku Park Tower rooftop and the atrium rooftop (measurement point 11, 2nd floor above ground). Moreover, six places (concrete ground in the sunshine, concrete ground in the shade, asphalt ground in the sunshine, grassland in the shade, building wall in the sunshine, and building wall in the shade) were chosen around measurement point 7, and the temperatures of the walls were measured with thermocouples.

3.2 Measurement Results

3.2.1 Total solar radiation

Figure 3 shows the total solar radiation during the measurement period. The solar radiation on the 20th was the lowest of the three days because it was cloudy. The highest value of 941W/m^2 was seen on the morning of August 21st; however it decreased rapidly in the afternoon as the weather became cloudy. The weather on the 22nd was steady, and a value of 700

W/m^2 from 10:00 to 13:00, a highest value of 820 W/m^2 at 11:00, and a value of 550 W/m^2 at 14:00 were recorded. From above results, it can be assumed that air conditioning systems were in full use on the 22nd, and thus the measurement results on the 22nd are focused on.

3.2.2 Wind velocity distribution

The velocity of the wind on the 22nd and the 21st tended to be higher than on the 20th, both on the rooftop and at each measurement point. This is because on a fine day in summer the atmosphere becomes unstable, and convection mixing becomes active. Moreover, it can be concluded that the velocity of the wind in the sky influenced the velocity of the wind at the ground, and so the direction of the wind varied widely on the 20th when the velocity of the wind in the sky was low. The velocities of the wind at 10:00, 13:00 and 15:00 on the 22nd are shown in Figures 4, 5, and 6 respectively. It can be seen that it was predominantly a south wind on the rooftop of the Shinjuku Park Tower. This tended towards the east at measurement point 3. This is thought to be because the south wind changed direction after running up against Shinjuku Park Tower, and entered the west side road at measurement point 3. The vortex formed on the leeward side of Shinjuku Park Tower at measurement point 7 generated a north wind. Moreover, measurement point 4 shows a stable south wind because it is situated along a south-north road.

3.2.3 Temperature and humidity distribution

Temperature and absolute humidity distributions at 10:00, 13:00 and 15:00 on the 22nd are shown in Figures 7, 8, and 9 respectively. Figure 10 shows the time history of the temperature and absolute humidity at measurement points 2 and 6 and the data from the Automated Meteorological Data Acquisition System (AMEDAS) in Otemachi, Tokyo. The temperature rose slowly in the morning, and there is virtually no decrease after 15:00. The temperatures were higher than the AMEDAS data in Otemachi. This is thought to be due to the influence of the high ground level temperature, because the measurement position is closer to central Tokyo than Otemachi. Absolute humidity rose in the morning, then decreased during the day, and tended to rise again in the evening. Little difference is shown on comparing the temperature and absolute humidity on the leeward side and the windward side of Shinjuku DHC Center. This indicates that the air-conditioning heat released from the cooling tower is assumed to be having no effect on the surrounding outdoor thermal environment. This will be also discussed in the simulation results.

3.2.4 Wall and ground temperature

As an overall tendency, the highest wall and ground temperature was shown at 13:00 from the results of the Infrared radiation thermometer. For example, on the 22nd, the ground temperature of measurement points 2, 3, and 5 reached about 45℃, and about 40℃ at measurement points 7 and 8. Moreover, point 2 showed the highest temperature. The reason is that the sunshine time at measurement point 2 was the longest. The temperature reached about 30℃ at a park near the DHC Center, about 42℃ on the road, and about 50 ℃ or more on the building rooftop from measurements on the rooftop of the Shinjuku Park Tower. Figure 11 shows the temperature of the wall around measurement point 7. The temperature of the asphalt is the highest, then the concrete ground, the building wall, and the grassland.

4. OUTLINE OF SIMULATION

4.1 Computational Grid

In order to simulate the thermal environment of a complex actual urban area, it is first necessary to obtain digital data that reproduces the shape of the three-dimensional urban area. In this study. three-dimensional city model data measured by an aircraft equipped with a laser scanner is used. In this data, the heights of buildings and trees are measured precisely by laser scanning from the aircraft. It is therefore highly-accurate digital data compared with traditional data in which the heights of buildings are calculated by the numbers of stories. As described in Section 2, it is necessary to make an unstructured computational grid from the above three-dimensional city model data to assess the outdoor thermal environment for this complex urban area. Three-dimensional city model data is first read by CAD software, then it is converted into Initial Graphics Exchange Specification (IGES) file format. Next, this IGES file is read by the computational grid making software (Gridgen), and an unstructured computational grid is made. Figure 12 shows the finished unstructured computational grid for the analysis area.

4.2 Simulation Conditions

The simulation object is shown in the frame

Fig. 12 Computational grids

Table 2 Analysis conditions

Turbulent model	Standard k-ε model
Difference scheme	Convection terms: MARS*
Inlet	$U = U_0 \cdot (Z/Z_0)^{1/4}, \quad Z_0 = 16m$ $k = 1.5 \cdot (I \times U)^2, \quad I = 0.1$ $\varepsilon = C_\mu \cdot k^{3/2}/l$ $l = 4(C_\mu \cdot k)^{1/2} Z_0^{1/4} Z^{3/4}/U_0$
Side, sky	Free slip
Wall	Generalized logarithmic law

*MARS: Monotone Advection and Reconstruction Scheme, second-order scheme (STAR-CD, 2001)
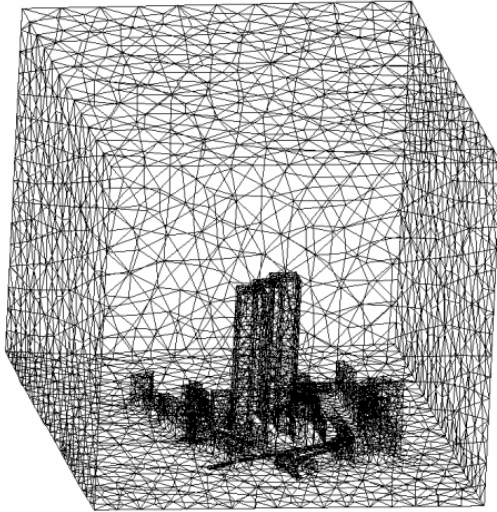
enclosed by broken lines in Figure 2. August 22nd 13:00 is targeted as the day for analysis. Total solar radiation is set at 701W/m^2 from the measurement result. The inflow velocity of the wind is set at 1/4th power profile, and the measurement value for the Shinjuku Park Tower rooftop (2.0m/s, southwest, and H=200m) is used as the representative velocity of the wind (U_0 in Table 2). The constant flux layer assumption is used to evaluate the turbulent kinetic energy. The average values of each measurement point are used for the initial temperature and humidity conditions. Table 2 shows details of the analysis conditions. The air-conditioning heat released from the DHC system is set to the design value of 200,000kW, and the ratio of sensible heat to latent heat is set at 1:9. The air-conditioning heat released from buildings that are not supplied by the DHC system (named individual buildings here) is obtained by the radiation and conduction coupled calculation. The ratio of sensible heat to latent heat is set at 6:4. The heat is set to be released from the rooftop for the individual buildings less than 40m in height. For the individual buildings of more than 40m in height, the released heat is divided into two equal parts, which are set to be released from the 30m height and ground respectively. Moreover, The velocity of the heat released from the cooling tower of the DHC system is set at 16.75m/s and upward, which is the value at the maximum operating time. SET* is calculated by the program based on the human-body heat balance model of Gagge et al. (1986). A two-node model is used, which incorporates an adjustment mechanism for perspiration. In calculating SET*, the amount of clothing and the metabolism of the human body are assumed as 0.5clo and 1.5met (this corresponds to wearing a short-sleeved shirt and trousers, and the

middle between slow walking and standing) respectively. Seppanen's equation is used to calculate the rate of average convection heat transfer for the human body. In this study, SET* is calculated using the temperature and the wetting rate of the skin after the human body is exposed for one hour to the thermal environment in summer.

5. COMPARISON OF RESULTS BETWEEN SIMULATION AND FIELD MEASUREMENT

5.1 Wind Velocity Distribution

Figure 13 shows the simulation results for the horizontal distribution of the wind velocity and the measurement results at a height of 1.5m. As an overall tendency, the simulation shows good agreement with the measurements. The velocity of the wind decreases close to the building, and a vortex is formed on the north side of the Shinjuku Park Tower (around measurement point 7). Moreover, the simulation values for the scalar wind velocity are 0.73m/s at point 3, 0.98m/s at points 4, and 0.89m/s at point 9; and the measured results are 0.94m/s, 1.09m/s, and 0.84 m/s respectively, which gives very good agreement. The vertical distribution in section A-A' (refer to Figure 2) is shown in Figure 14. It shows that a strong rising flow is formed by the influence of the upward blow from the cooling tower.

5.2 Temperature and Absolute Humidity Distribution

The horizontal distributions of temperature and absolute humidity at a height of 1.5m are shown in Figures 15 and 16. It can be seen that the temperature
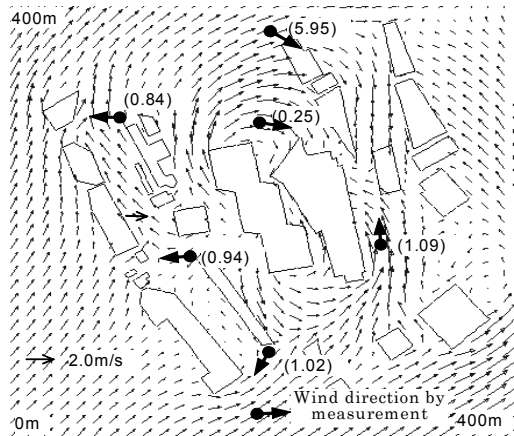
Fig.13 Horizontal wind distribution (m/s)(1.5m Height)
( ) measurement data
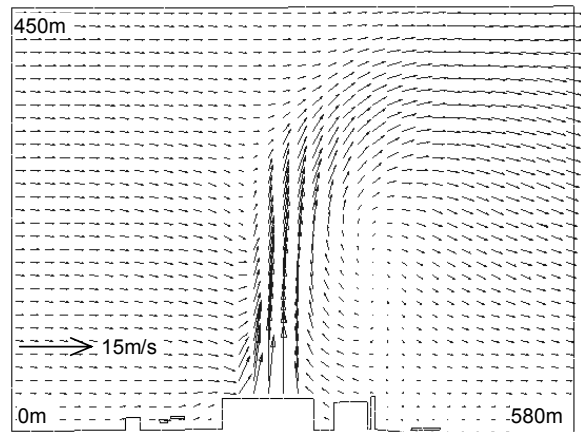
Fig.14 Vertical wind distribution (m/s) (A-A' section)
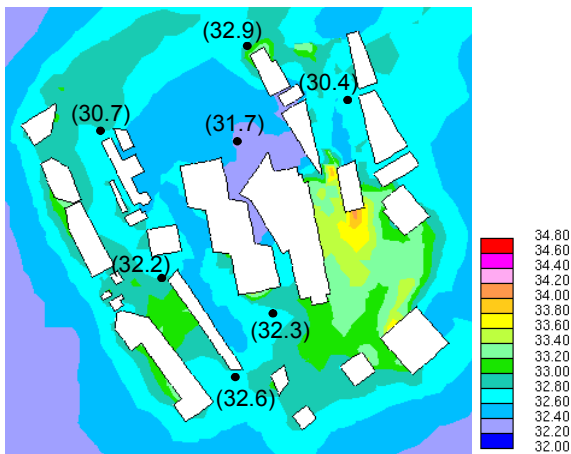
Fig.15 Horizontal temperature distribution (℃)
( ) measurement data (1.5m Height)
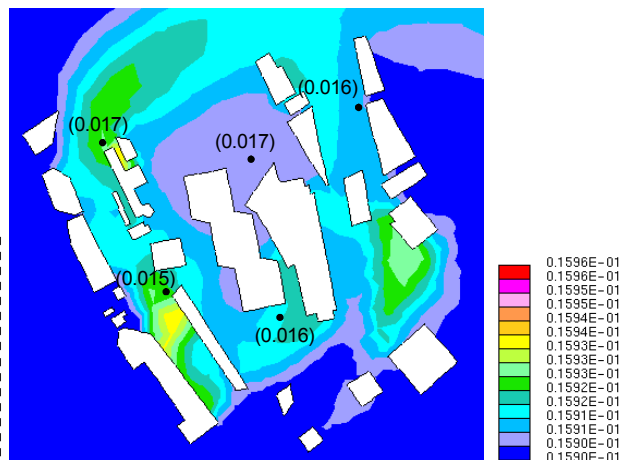
Fig.16 Horizontal absolute humidity distribution (kg/kg')
( ) measurement data (1.5m Height)

Fig.17 Vertical temperature distribution (℃)
(A-A' section)
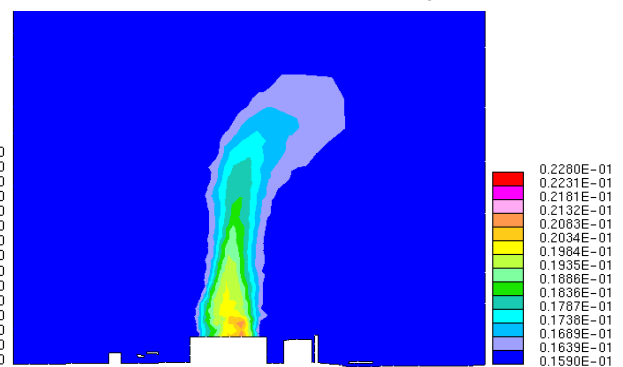
Fig.18 Vertical absolute humidity distribution (kg/kg')
(A-A' section)

and absolute humidity are high around the measurement points close to the buildings and the places where the velocity of the wind is weak. We can see that the measurement results and the simulation results are in good agreement. The vertical distribution at section A-A ' is shown in Figures 17 and 18. It is thought that there is little influence on the ground because the heat and vapor are blown from the cooling tower high up into the sky. This gives

agreement with the measurement result that there is little difference between the temperature and humidity on the windward side and the leeward side of the area.

5.3 SET * Distribution

Figure 19 shows the horizontal distribution of SET * at a height of 1.5m. It shows 32℃ or more in the analysis area, and a high value of 39℃ appears
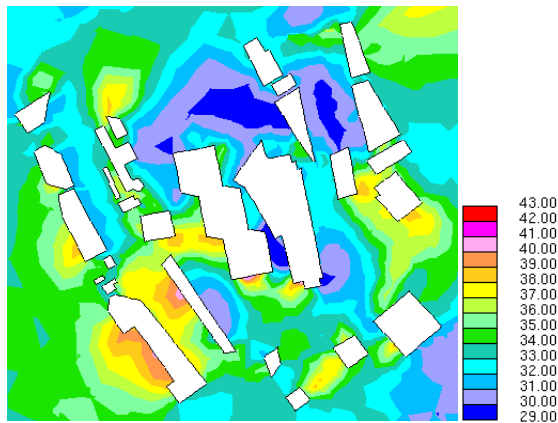
Fig.19 SET* distribution (℃) (1.5m Height)

locally, especially at the places where the velocity of the wind is weak or in the sunshine.

6. CONCLUSIONS

The total solar radiation, temperature, humidity, and velocity of the wind were measured around the Shinjuku DHC Center in summer, and the influence of the heat released from the cooling towers on the surrounding thermal environment was evaluated. There is no significant difference on comparing the thermal environment on the windward and leeward sides of the DHC system. An outdoor thermal environment simulation tool coupled with convection, radiation and conduction, and which is adapt to the complex urban area was developed. Comparing the measurement results and the simulation results for temperature, humidity and wind velocity confirmed that this tool is effective in assessment of the outdoor thermal environment. Moreover, it is thought that the cooling towers have little influence on the surrounding thermal environment because the sensible heat and the latent heat are blown away high up into the sky.

References

Gagge, A. P., Stolwijk, J. A. J., Nishi, Y., 1986, A standard predictive index of human respons to the thermal environment, AHSRAE Transactions, 92,1, 709-731

Harayama, K., Yoshida, S., Ooka, R., Mochida, A., Murakami, S., 2002, Prediction of outdoor environment with unsteady coupled simulation of convection, radiation and conduction, Part 1, Numerical study based on unsteady radiation and conduction analysis, J. Archit. Plann. Environ. Eng., AIJ, 556, 99-106 (in Japanese)

Omori, T., Yang, J., Kato, S., Murakami, S., 2003, Radiative heat transfer analysis method for coupled simulation of convection and radiation in large-scale and complicated enclosures, Part 1, Accurate radiative heat transfer analysis based on Monte Carlo Method, *Transactions of the Society of Heating, Air-Conditioning and Sanitary Engineers of Japan*, 88, 103-113 (in Japanese)

STAR-CD. Methodology, STAR-CD Version 3.15. Computational Dynamics Limited, 2001

Yoshida, S., Murakami, S., Mochida, A., Ooka, R., Tominaga, Y., Kim, S., 2000a, Influence of green area ratio on outdoor thermal environment with coupled simulation of convection, radiation and moisture transport, *J. Archit. Plann. Environ. Eng., AIJ*, 529, 77-84 (in Japanese)

Yoshida, S., Ooka, R., Mochida, A., Tominaga, Y., Murakami, S., 2000b, Study on effect of greening on outdoor thermal environment using three dimensional plant canopy model, *J. Archit. Plann. Environ. Eng., AIJ,* 536, 87-94 (in Japanese)